Cellular/Molecular

A Signaling Mechanism from Gαq-Protein-Coupled Metabotropic Glutamate Receptors to Gene Expression: Role of the c-Jun N-Terminal Kinase Pathway

Lu Yang,[1] Limin Mao,[1] Hai Chen,[1] Michael Catavsan,[1] Jonathan Kozinn,[2] Anish Arora,[1] Xianyu Liu,[1] and John Q. Wang[1,2]

Departments of [1]Basic Medical Science and [2]Anesthesiology, University of Missouri–Kansas City School of Medicine, Kansas City, Missouri 64108

Gαq-protein-coupled group I metabotropic glutamate receptors (mGluRs) are densely expressed in brain neurons and are actively involved in various cellular activities. In this study, we investigated the role of group I mGluRs in regulating the c-Jun N-terminal kinase (JNK)/stress-activated protein kinase in cultured neurons. We found that selective activation of mGluR5 induced a rapid and transient phosphorylation of JNK. In a series of studies to determine the mechanisms, we found that the conventional mGluR5-associated signaling pathways (inositol-1,4,5-triphosphate-mediated Ca^{2+} release and activation of protein kinase C) were not involved in the mGluR5 regulation. Instead, ligand stimulation of mGluR5 caused a dynamic transactivation of the epidermal growth factor (EGF) receptor, which in turn triggered a downstream signaling pathway to upregulate JNK phosphorylation. Furthermore, the mGluR5-dependent JNK activation specifically activated c-Jun, but not activating transcription factor-2 or JunD, and increased activator protein-1 (AP-1)-mediated endogenous transcriptional activity. Together, we identified a novel mGluR5-to-nucleus communication through the EGF/JNK pathway, which functions to regulate AP-1-mediated transcription.

Key words: mGluR; MAPK; JNK; SAPK; Jun; MKK; AP-1; EGF; striatum; nucleus accumbens

Introduction

Group I metabotropic glutamate receptors (mGluRs) are distributed in broad areas of the brain, including the two striatal structures of basal ganglia: the caudate–putamen and the nucleus accumbens (Testa et al., 1994; Tallaksen-Greene et al., 1998). Emerging evidence has indicated that these receptors in the striatum are actively involved in the regulation of normal and abnormal cellular activities related to motor, neurodegenerative, psychiatric, and cognitive disorders (for review, see Wang et al., 2003). Two subtypes of group I mGluRs (mGluR1 and mGluR5) are positively coupled to phosphoinositide (PI) hydrolysis through Gαq proteins (Nakanishi, 1994; Conn and Pin, 1997). Agonist binding of these subtypes results in an increase in hydrolysis of membrane PI via activating phospholipase Cβ1 (PLCβ1). This yields diacylglycerol (DCG), which activates protein kinase C (PKC), and inositol-1,4,5-triphosphate (IP₃), which releases intracellular Ca^{2+} ($[Ca^{2+}]_i$). Altered PKC and Ca^{2+} signals could then engage in the modulation of various downstream metabotropic activities.

Mitogen-activated protein kinases (MAPKs) refer to a large family of cytosolic and nuclear serine/threonine protein kinases that are expressed in postmitotic neurons of adult mammalian brain and function in regulating cell survival, synaptic plasticity, inducible gene expression, and many other activities (Nozaki et al., 2001; Pearson et al., 2001). The first subfamily of MAPKs was identified as extracellular signal-regulated kinases (ERKs) with many isoforms (ERK1/2/3/4/5/7) (Peyssonnaux and Eychene, 2001; Volmat and Pouyssegur, 2001). At least two additional subfamilies of MAPKs have been identified: the c-Jun N-terminal kinase(JNK)/stress-activated protein kinase (SAPK) and p38 MAPKs (Nozaki et al., 2001; Gallo and Johnson, 2002). All three subfamilies of MAPKs are activated through threonine and tyrosine phosphorylation by the upstream MAPK kinase (MKK). However, these MAPKs are very heterogeneous in their phosphorylation sites, upstream MKKs, downstream substrates, and thus physiological functions.

L-glutamate (glutamate) is a major excitatory neurotransmitter in the brain and is among effective extracellular signals that readily activate MAPKs in striatal neurons *in vivo* and *in vitro* (for review, see Wang et al., 2004). Agonist ligands for ionotropic glutamate receptors (NMDA or AMPA) or for group I mGluRs increased striatal ERK1/2 phosphorylation via distinct signaling mechanisms involving Ca^{2+}-sensitive or Ca^{2+}-insensitive kinases (Sgambato et al., 1998; Perkinton et al., 1999, 2002; Vanhoutte et al., 1999; Thandi et al., 2002; Mao et al., 2004, 2005a; Yang et al., 2004). Similarly, glutamate increased JNK phosphorylation on their Thr[183] and Tyr[185] sites in striatal neurons (Schwarzschild et al., 1997; Mukherjee et al., 1999; Vanhoutte et al., 1999; Crossthwaite et al., 2004). However, to date, the regu-

lation of JNK phosphorylation by mGluRs, particularly group I receptors, has not been described in neurons.

We therefore examined the role of group I mGluRs in regulating JNK phosphorylation in cultured striatal neurons. We found that selective mGluR5 activation induced a rapid and transient JNK phosphorylation. The JNK phosphorylation was mediated through a dynamic transactivation of the epidermal growth factor (EGF) receptor. Active JNK induced a discrete profile of transcriptional activation. Together, mGluR5 activates an efficient JNK-mediated synapse-to-nucleus communication for the regulation of gene expression.

Materials and Methods

Primary striatal neuronal cultures. Standardized procedures in this laboratory were used to prepare primary striatal neuronal cultures from 18-d-old rat embryos (Charles River, New York, NY) (Yang et al., 2004; Mao et al., 2005a,b). Predominant GABAergic neurons were obtained using the procedures as evidenced by the fact that >90% of total cells were immunoreactive to glutamic acid decarboxylase-65/67, GABA, and the specific marker for neurons [microtubule-associated protein-2a + 2b (MAP2)] but not for glia (glial fibrillary acidic protein). Cells were cultured for 14–16 d before use.

Transient transfection and luciferase reporter assay. To monitor the transcription mediated by activator protein-1 (AP-1), we used a pAP1-Luc reporter plasmid (Clontech, Palo Alto, CA) containing four tandem copies of the AP-1 core consensus sequence fused to the sequence coding the firefly luciferase gene. Transfections of the plasmid (1 μg/well) into cultured striatal neurons were performed using the cationic lipid Lipofectamine 2000 (Invitrogen, Carsbad, CA) by following an optimized procedure described previously (Yang et al., 2004; Mao et al., 2005a). Eighteen hours after the transfection, cells were treated with the indicated agents, harvested with 1$\times$ reporter lysis buffer (Promega, Madison, WI) into 1.5 ml tubes on ice, and assayed for luciferase activity by adding the substrate luciferin of luciferase from a luciferase reporter assay kit (Promega). Relative light units (RLUs) were measured using a Turner Luminometer (Promega). The promoterless luciferase vector pTAL-Luc (Clontech) was included in every experiment so that its minor luciferase signal, if there is any, could be subtracted from activity driven by AP-1 constructs. Overall transfection efficiency was determined by nuclear DNA staining with 4′,6-diaminino-2-phenylindole after transfection of a pCMS-enhanced green fluorescent protein (EGFP) vector (Clontech). We found no difference in transfection efficiency among wells that were treated with the same experimental procedures. All experiments were performed in triplicate.

Western blot analysis. Cell lysates from cultures were sonicated, and protein concentrations were determined. An equal amount of protein (20 μg/20 μl/lane) was separated on SDS NuPAGE Novex (Wadsworth, OH) 4–12% gels (Invitrogen). Proteins were transferred to polyvinylidene fluoride membrane (Millipore, Bedford, MA) and blocked in blocking buffer (5% nonfat dry milk in PBS and 0.1% Tween 20) for 1 h. The blots were incubated in primary rabbit polyclonal antibodies against pERK1/2(Thr^{202}/Tyr^{204}), ERK1/2, pERK5(Thr^{218}/Tyr^{220}), ERK5, pJNK(Thr^{183}/Tyr^{185}), JNK, p-p38(Thr^{180}/Tyr^{182}), p38, p-c-Jun(Ser^{63}), p-c-Jun(Ser^{73}) also detecting pJunD(Ser^{100}), c-Jun (all from Cell Signaling Technology, Beverly, MA), JunD (Santa Cruz Biotechnology, Santa Cruz, CA), pATF-2(Thr^{71}) (Cell Signaling Technology), ATF-2 (Cell Signaling Technology), pMKK4(Ser^{80}) (Cell Signaling Technology), MKK4 (Cell Signaling Technology), phospho-EGF receptor(Tyr^{1173}) (Cell Signaling Technology), EGF receptors (Cell Signaling Technology), or β-actin (Santa Cruz Biotechnology) usually at 1:500–1000 overnight at 4°C. This was followed by 1 h of incubation in goat anti-rabbit horseradish peroxidase-linked secondary antibodies (Jackson ImmunoResearch, West Grove, PA) at 1:5000. Immunoblots were developed with the enhanced chemiluminescence reagents (Amersham Biosciences, Piscataway, NJ) and captured into Kodak (Rochester, NY) Image Station 2000R. Kaleidoscope-prestained standards (Bio-Rad, Hercules, CA) were used for protein size determination. The density of immunoblots

was measured using the Kodak 1D Image Analysis software, and all bands were normalized to percentages of control values.

Immunofluorescent labeling. Single or double immunofluorescent labeling on eight-chamber coverslip slides was performed as described previously (Yang et al., 2004; Mao et al., 2005a). Briefly, cultures were fixed in cold 4% paraformaldehyde (10 min), followed by incubation in 4% normal donkey serum and 1% bovine serum album (20 min) to block nonspecific staining. The cells were treated with primary antibodies usually at 1:250–500 for one to two nights at 4°C. Slides were then incubated for 1 h with donkey secondary antibodies conjugated to FITC or tetramethylrhodamine isothiocyanate (Jackson ImmunoResearch) at 1:200. The immunofluorescent images were analyzed using confocal microscopy (Nikon C1 laser scanning confocal microscope; Nikon, Tokyo, Japan).

Coimmunoprecipitation. Rat striatal cell proteins were prepared under weakly denaturing conditions to permit the protein/protein interaction (Takagi et al., 2000). Briefly, striatal cultures were scraped into a microtube containing ice-cold sample buffer (in mM: 10 Tris-HCl, pH 7.4, 5 NaF, 1 Na$_3$VO$_4$, 1 EDTA, and 1 EGTA) and homogenized by sonication. The homogenate was centrifuged at 800 $\times$ g (15 min) at 4°C. The supernatant was again centrifuged at 11,000 $\times$ g at 4°C for 30 min to obtain the P2 pellet, a fraction enriched with synaptic structures. The P2 pellet was resuspended in sample buffer and solubilized in 1% sodium deoxycholate. After incubation at 37°C for 30 min, Triton X-100 was added to a final concentration of 0.1%. Insoluble proteins were sedimented at 100,000 $\times$ g for 20 min at 4°C. The supernatants were used for coimmunoprecipitation. mGluR5 and EGF receptors were then precipitated using rabbit antibodies against mGluR5 (Upstate Biotechnology, Charlottesville, VA) and EGF receptors (Cell Signaling Technology), respectively, and 50% protein A agarose/Sepharose bead slurry (Amersham Biosciences). Proteins were separated on Novex 4–12% gels and probed with rabbit antibodies against mGluR5 (Upstate Biotechnology) or EGF receptors (Cell Signaling Technology). HRP-conjugated secondary antibodies and enhanced chemiluminescence were used to detect proteins. Negative controls with antigen preabsorption were performed for antibodies used in immunoprecipitation.

Immune-complex MAPK activity assays. MAPK activity was measured with nonradioactive assay kits according to the protocol of the manufacturer (Cell Signaling Technology). Briefly, cells were lysed in ice-cold cell lysis buffer (20 mM Tris, pH 7.5, 150 mM NaCl, 1 mM EDTA, 1 mM EGTA, 1% Triton X-100, 2.5 mM sodium pyrophosphate, 1 mM glycerol phosphate, 1 mM Na$_3$VO$_4$, 1 μg/ml leupeptin, and 1 mM phenylmethylsulfonyl fluoride). Equal volumes of cell lysates (300 μg) were incubated with c-Jun fusion protein beads, immobilized phospho-ERK monoclonal antibody, and immobilized phospho-p38 monoclonal antibody for JNK, ERK, and p38, respectively, at 4°C overnight. After centrifugation, pellets were suspended in kinase buffer (25 mM Tris, pH 7.5, 5 mM glycerol phosphate, 2 mM dithiothreitol, 0.1 mM Na$_3$VO$_4$, 10 mM MgCl$_2$, and 200 μM ATP) and then immunoprecipitated with the specific fusion protein c-Jun, Elk-1, and activating transcription factor-2 (ATF-2) for JNK, ERK, and p38, respectively, at 30°C for 30 min. The activity of JNK, ERK, and p38 was then measured by Western blot with a 1:1000 dilution of primary antibodies [rabbit polyclonal p-c-Jun(Ser^{63}), pElk-1(Ser^{383}), pATF-2(Thr^{71}) antibodies] as described above (see Western blot analysis).

PI hydrolysis. PI hydrolysis was analyzed by measuring the concentration of IP$_3$ with the IP$_3$ assay supplement kit from PerkinElmer (Palo Alto, CA) according to instructions of the manufacturer. Briefly, cultures were washed with HEPES-buffered balanced salt solution (in mM: 154 NaCl, 5.6 KCl, 2 CaCl$_2$, 2 MgSO$_4$, 5.5 glucose, and 20 HEPES-KOH or HEPES-NaOH, pH 7.4) and incubated in this solution. (RS)-3,5-dihydroxyphenylglycine (DHPG) was added for 0.5–1 min. After drug treatment, the solutions were aspirated, and ice-cold methanol was added to terminate the reaction. Cells were scraped and briefly sonicated before the aqueous and organic phases were separated by centrifugation at 4000 rpm for 10 min. The upper aqueous phase was analyzed for the concentration of IP$_3$ with an addition of glutathione S-transferase (GST)-tagged IP$_3$ binding protein followed by an addition of detection mix containing biotinylated IP$_3$ analog, streptavidin-coated donor beads, and anti-GST conjugated acceptor beads.
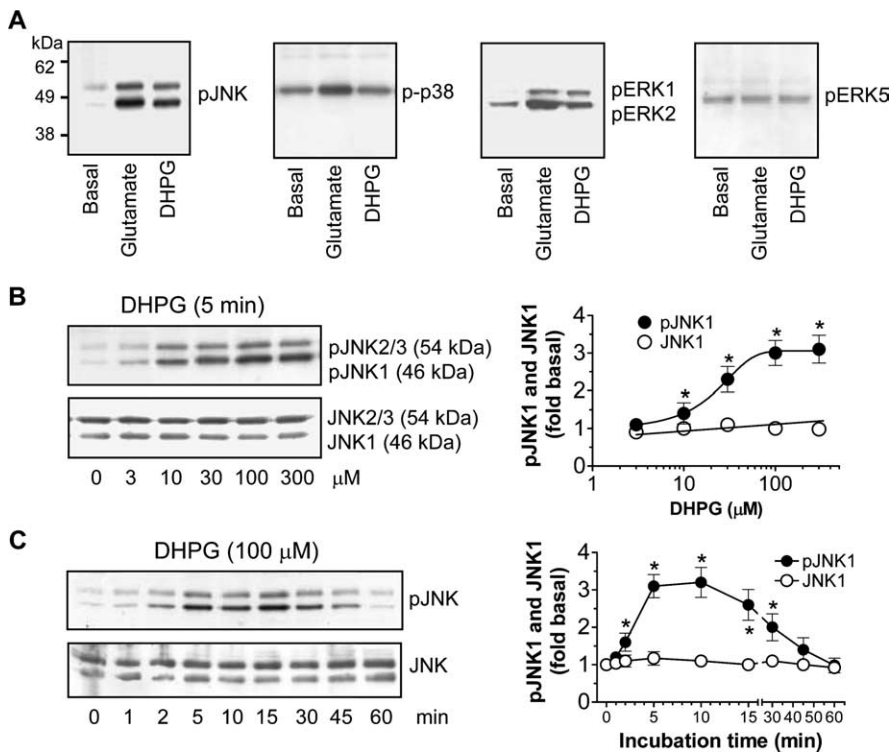
Figure 1. JNK phosphorylation by activation of group I mGluRs with DHPG in cultured rat striatal neurons. *A*, Effects of glutamate and DHPG on basal levels of phosphorylated JNK, p38, ERK1/2, and ERK5. Glutamate (50 μM) or DHPG (100 μM) was incubated for 5–10 min. Both glutamate and DHPG increased JNK phosphorylation. *B*, A dose–response study illustrating a concentration-dependent increase in pJNK, but not JNK, levels in response to DHPG incubation at different concentrations (3–300 μM; 10 min). Representative immunoblots are shown left of the quantified data of pJNK1 and JNK1 analyzed from separate experiments (mean $\pm$ SEM; $n = 5$). *C*, A time course study illustrating a rapid and transient increase in JNK phosphorylation, without changes in JNK levels, after DHPG incubation at 100 μM for different durations. Representative immunoblots are shown left of the quantified data (mean $\pm$ SEM; $n = 5$). *$p < 0.05$ versus basal levels.

$[Ca^{2+}]_i$ *measurements.* $[Ca^{2+}]_i$ measurements were performed with fura-2 AM fluorescence according to our previous procedures (Mao and Wang, 2002; Yang et al., 2004). The $[Ca^{2+}]_i$ concentration was calculated from ratios of the intensities of emitted fluorescence at two excitation wavelengths (F340/F380) with Northern Eclipse Image software (Empix Imaging, Mississauga, Ontario, Canada). When needed, fluorescence ratios (340/380) were converted to an absolute $[Ca^{2+}]_i$ concentration using the equation: $[Ca^{2+}]_i = K_d(F_{min}/F_{max})[(R - R_{min})/(R_{max} - R)]$.

Cell viability assay. Cell viability was measured using a double fluorescein diacetate/propidium iodide staining procedure (Jones and Senft, 1985). Cells were rinsed twice with 1× PBS and incubated PBS (0.5 ml/per well) containing 10 μg/ml fluorescein diacetate (Sigma, St. Louis, MO) and 5 μg/ml propidium iodide (Sigma). Cultures were washed once with PBS and examined under fluorescent light microscopy. The total numbers of viable cells stained by green fluorescein and dead cells stained by red propidium iodide were determined by counting cells in five random fields. Positive control was produced by treating cultures with kainic acid (500–1000 μM; 24 h)

Materials and drug treatments. NMDA, (+)-5-methyl-10,11-dihydro-5*H*-dibenzo[a,d]cyclohepten-5,10-imine maleate (MK-801), DL-2-amino-5-phosphonovaleric acid (AP-5), AMPA, 4-(8-methyl-9*H*-1,3-dioxolo[4,5-h][2,3]benzodazepin-5-yl)-benzenamine dihydrochloride (GYKI52466), 6,7-dinitroquinoxaline-2,3-dione (DNQX), DHPG, (*RS*)-2-chloro-5-hydroxyphenylglycine (CHPG), 2-methyl-6-(phenylethynyl)pyridine hydrochloride (MPEP), 7-(hydroxyimino)cy-clo-propa[b]chromen-1*a*-carboxylate ethyl ester (CPCCOet), nifedipine, thapsigargin, and anthra[1,9-*cd*]pyrazol-6(2*H*)-one (SP600125) were purchased from Tocris Cookson. U73122, U73343, 3-[1-3-(amidinothio)-propyl-1*H*-indol-3-yl]-3-(1-methyl-1*H*-indol-3-yl)maleimide (Ro-31-8220), AG1478, and AG825 were purchased from Calbiochem (La Jolla,

CA). L-Glutamate, 2,5-dimethyl-4-[2-(phenylmethyl)benzoyl]-1*H*-pyrrole-3-carboxylic acid methylester (FPL64176), tetrodotoxin (TTX), 2-[1-(3-dimethylaminopropyl)-5-methoxyindol-3-yl]-3-(1*H*-indol-3-yl)maleimide (Gö6983), phorbol 12-myristate 13-acetate (PMA), and dopamine were purchased from Sigma. Fura-2 AM, BAPTA-AM, and calcium green-1/AM were purchased from Invitrogen (Eugene, OR). Recombinant human EGF was purchased from Invitrogen. Drug treatments were made according to a procedure described previously (Yang et al., 2004; Mao et al., 2005).

Statistics. The results are presented as mean $\pm$ SEM and were evaluated using a one- or two-way ANOVA, as appropriate, followed by a Bonferroni's (Dunn) comparison of groups using least squares-adjusted means. Probability levels of <0.05 were considered statistically significant.

Results

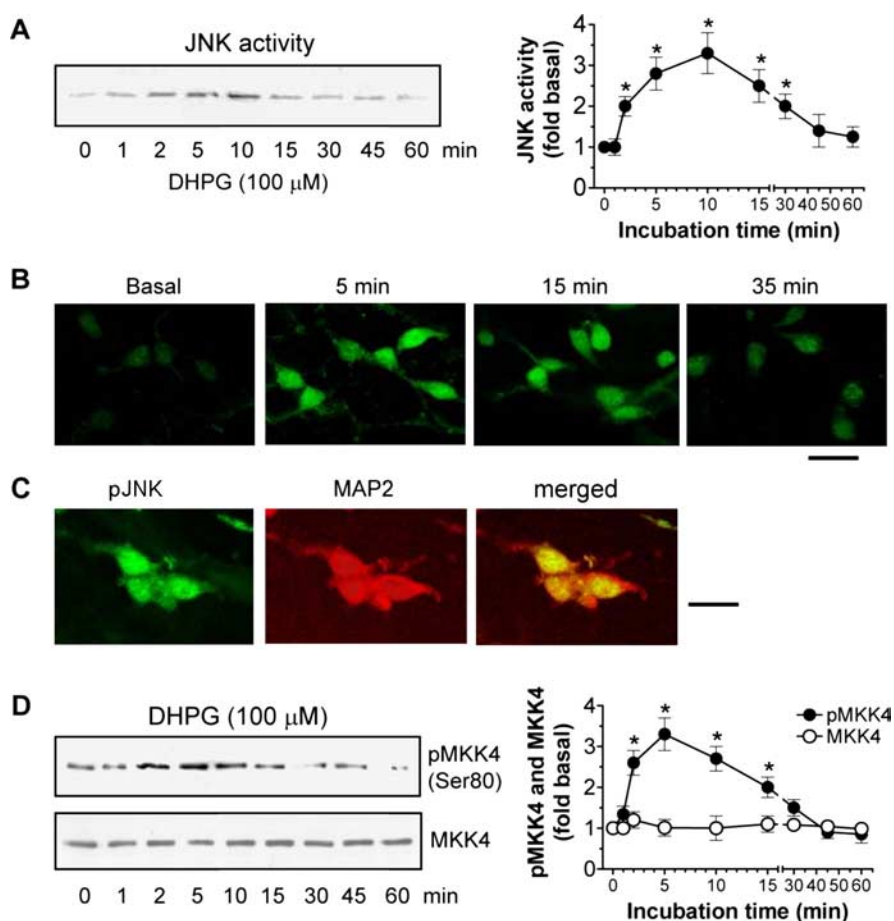### Activation of group I mGluRs increases JNK phosphorylation

We first set out to screen the effect of glutamate and the group I mGluR agonist DHPG on basal phosphorylation of three major MAPK subclasses (JNK, p38, and ERK) in cultured striatal neurons. We found that glutamate (50 μM; 5–10 min) elevated basal levels of pJNK, *p*-p38, and pERK1/2 but not pERK5 (Fig. 1*A*). Similarly, DHPG (100 μM; 5–10 min) consistently increased pJNK and pERK1/2 levels (Fig. 1*A*). However, DHPG did not alter basal levels of *p*-p38 and pERK5. Both glutamate and DHPG had no effects on cellular levels of JNK, p38, ERK1/2, and ERK5 (data not shown). These data demonstrated a positive linkage from group I mGluRs to JNK phosphorylation. We then performed a dose-responsive and a time course study to characterize the group I mGluR-regulated JNK phosphorylation. At a low concentration (3 μM), DHPG did not alter basal pJNK levels (Fig. 1*B*). At 10 μM, DHPG significantly increased pJNK levels. A greater increase in pJNK levels was seen at higher concentrations (30–300 μM). No significant changes were seen in cellular levels of JNK after DHPG application at all concentrations surveyed. These data showed a clear dose-dependent increase in JNK phosphorylation after activation of DHPG-sensitive group I mGluRs. In the time course study in which DHPG at 100 μM was added to cultures for different durations, a rapid and transient increase in JNK phosphorylation with a peak time of ~5–10 min occurred with no changes in JNK levels (Fig. 1*C*). A different time course evaluation was also performed, in which 100 μM DHPG was incubated for 2 min, and cultures were then lysed 3, 8, 30, or 60 min after the termination of DHPG incubation. The data from this study (data not shown) were similar to those obtained by the DHPG incubation at different durations. DHPG might cause a release of an assortment of transmitters and modulators in the culture, leading to activation of receptors other than group I mGluRs to account for the observed changes in JNK phosphorylation in striatal neurons. However, this possibility seems less likely because TTX (1 μM), a Na$^+$ channel blocker blocking presynaptic action potentials and thus transmitter releases, did not effect the DHPG-induced JNK

phosphorylation (Fig. S1, available at www.jneurosci.org as supplemental material). There was no significant difference in cell viability between control and DHPG-treated cultures as detected by the double fluorescein diacetate-propidium iodide staining.

Phosphorylation of JNK leads to activation of this kinase (Nozaki et al., 2001; Gallo and Johnson, 2002). Consistent with this, DHPG (100 μM) increased basal levels of JNK activity, which kinetically paralleled with dynamic increases in JNK phosphorylation after DHPG application (compare Figs. 2A and 1C). To define the subcellular distribution of activated pJNK, single immunofluorescent labeling was performed on cultures treated with DHPG (100 μM; 10 min). Strong immunostaining of pJNK was revealed within the nucleus and weak to moderate staining in the cytoplasm and neural processes (Fig. 2B). In addition, in double immunofluorescent labeling, pJNK-positive neurons were immunoreactive to the neuron-specific marker MAP2 (Fig. 2C), indicating that JNK phosphorylation by DHPG occurred in neuronal cells. MAPK kinase 4 (MKK4) is an upstream kinase of JNK. DHPG may activate MKK4 to increase JNK phosphorylation. To examine this idea, phosphorylation of MKK4 at serine 80 was detected in cultures stimulated by DHPG. It was found that DHPG (100 μM) induced a rapid and transient increase in pMKK4 levels (Fig. 2D), which closely corresponded with the kinetics of DHPG-stimulated JNK phosphorylation. This indicates that MKK4 may serve as an upstream kinase responsible for the phosphorylation of its substrate JNK.

Figure 2. Effects of activation of group I mGluRs with DHPG on JNK activity (**A**), pJNK immunostaining (**B**, **C**), and MKK4 phosphorylation (**D**) in cultured rat striatal neurons. **A**, A time course study illustrating a rapid and transient increase in JNK activity after DHPG incubation at 100 μM for different durations. Representative immunoblots of phospho-c-Jun(Ser[63]) defined as JNK activity are shown left of the quantified data (mean ± SEM; $n = 4$). **B**, Confocal immunofluorescent images illustrating subcellular distributions of pJNK in response to DHPG stimulation (100 μM; 5–35 min). Strong pJNK immunostaining (green) was seen in the nucleus and weak to moderate staining in the cytoplasm and neural processes. Scale bar, 30 μm. **C**, Confocal immunofluorescent images illustrating coexpression of pJNK (green) with a neuronal specific marker MAP2 (red) in cultures treated with DHPG (100 μM; 10 min). Scale bar, 20 μm. **D**, A time course study illustrating a rapid and transient increase in MKK4 phosphorylation after DHPG incubation at 100 μM for different durations. No change was observed in basal levels of MKK4. Representative immunoblots are shown left of the quantified data (mean ± SEM; $n = 5$). *$p < 0.05$ versus basal levels.

DHPG-induced JNK phosphorylation is independent on NMDA and AMPA receptors and Ca^{2+} channels

NMDA receptors may contribute to the DHPG effect. To explore this possibility, we evaluated the effect of the NMDA receptor-selective antagonists on the DHPG-stimulated JNK phosphorylation. Pretreatment with the noncompetitive NMDA receptor antagonist MK-801 at 1 μM, a dose sufficient to block the NMDA-induced JNK phosphorylation, did not change the JNK phosphorylation induced by DHPG (Fig. S2A, available at www. jneurosci.org as supplemental material). Studies with the competitive NMDA receptor antagonist AP-5 (50 μM) produced the similar results (data not shown). Thus, NMDA receptors are less likely involved in the DHPG effect. To determine the role of AMPA receptors, the AMPA receptor antagonist GYKI52466 (50–100 μM) was used, and we found that GYKI52466 did not block the JNK phosphorylation induced by DHPG, whereas GYKI52466 blocked the AMPA-induced JNK phosphorylation (Fig. S2B, available at www.jneurosci.org as supplemental material), and neither did another AMPA receptor antagonist DNQX at 100 μM, a dose sufficient to block the AMPA phosphorylation

of JNK (data not shown). Thus, like NMDA receptors, AMPA receptors are not important in mediating the DHPG effect. Finally, the L-type voltage-operated Ca^{2+} channel (VOCC) was investigated for its importance. We found that the VOCC-selective inhibitor nifedipine at 20 μM, which was effective to block the VOCC activator FPL64176-stimulated JNK phosphorylation, did not alter the hyperphosphorylation of JNK induced by DHPG (Fig. S2C, available at www.jneurosci.org as supplemental material). This suggests that the VOCC is not a significant component in the DHPG phosphorylation of JNK.

mGluR5 mediates DHPG-induced JNK phosphorylation

Because DHPG has a spectrum of activating both group I mGluR subtypes (mGluR1 and 5), a series of studies was performed to identify the subtype that mediates the DHPG effect. Pretreatment of cultured striatal neurons with the noncompetitive mGluR1-selective antagonist CPCCOet (1 or 5 μM) did not significantly alter the DHPG-stimulated JNK phosphorylation (Fig. 3A). In contrast, the noncompetitive mGluR5-selective antagonist MPEP at the same concentrations blocked JNK phosphorylation (Fig. 3B). The mGluR5-selective agonist CHPG (1–2 mM; 10
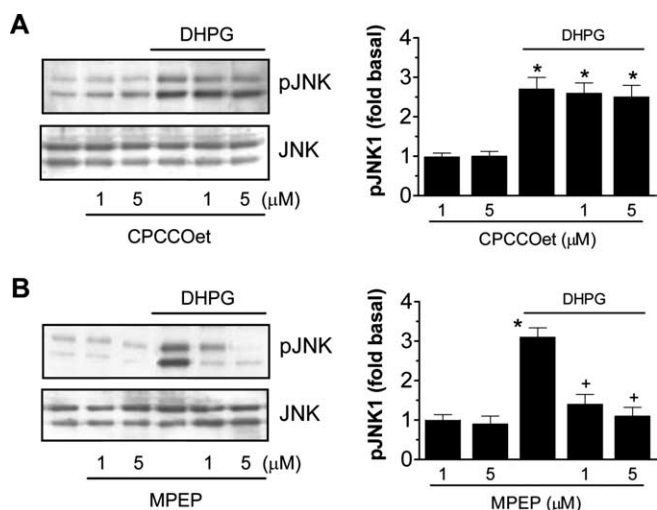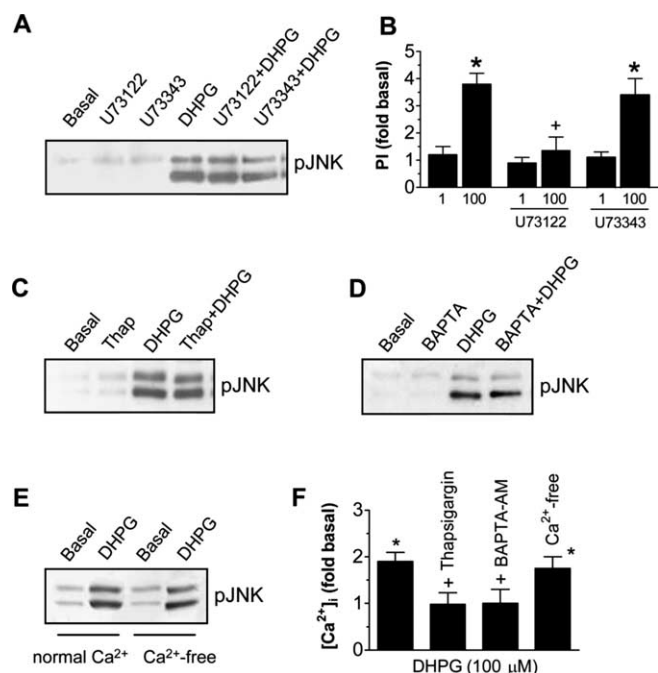
Figure 3. Effects of the antagonist selective for mGluR1 (CPCCOet; **A**) or mGluR5 (MPEP; **B**) on basal and DHPG-induced JNK phosphorylation in cultured rat striatal neurons. CPCCOet (1 or 5 μM) or MPEP (1 and 5 μM) was incubated 30 min before and during a 10 min treatment with DHPG (100 μM). Note that MPEP blocked, whereas CPCCOet had no effect on, the DHPG-induced JNK phosphorylation. Representative immunoblots are shown to the left of the quantified data of pJNK1. Values are expressed in terms of mean ± SEM ($n = 4–6$). *$p < 0.05$ versus basal levels. +$p < 0.05$ versus DHPG alone.


Figure 4. The contribution of the mGluR5-associated signaling pathway to the JNK phosphorylation induced by DHPG in cultured rat striatal neurons. **A**, Pretreatment of striatal neurons with the PLCβ1 inhibitor U73122 did not reduce the JNK phosphorylation induced by DHPG ($n = 4$). **B**, U73122, but not U73343, totally blocked the increases in PI hydrolysis induced by DHPG ($n = 3–5$). U73122 or U73343 at 40 μM was incubated 30 min before DHPG (100 μM) for 10 min (**A**) or 0.5–1 min (**B**). **C**, Thapsigargin (Thap) did not reduce the JNK phosphorylation induced by DHPG ($n = 4$). **D**, The Ca^{2+} chelator BAPTA-AM had no effect on JNK phosphorylation ($n = 5$). **E**, DHPG (100 μM; 10 min) induced a comparable increase in JNK phosphorylation in either Ca^{2+}-containing or Ca^{2+}-free medium ($n = 4–5$). **F**, Thapsigargin and BAPTA-AM completely blocked intracellular Ca^{2+} rises induced by DHPG (100 μM). In **C**, **D**, and **F**, thapsigargin (2 μM) or BAPTA-AM (30 μM) was incubated 1 h before and during a 10 min treatment with DHPG (100 μM). Values in **F** are expressed as mean-fold changes of basal levels in terms of the peak amplitude of Ca^{2+} responses measured within 1 min after the start of DHPG treatment from 16 to 24 neurons. *$p < 0.05$ versus basal levels. +$p < 0.05$ versus DHPG (100 μM) alone.

min) induced an increase in pJNK to an extent comparable with that induced by DHPG (100 μM), and the CHPG-induced JNK phosphorylation was sensitive to MPEP (1 μM) but not CPCCOet (5 μM; data not shown). Immunoblots prepared with JNK antibody showed again that changes in the JNK phosphorylation were not attributable to changes in total JNK proteins. The above data provide evidence that mGluR5, rather than mGluR1, is a subtype responsible for mediating the DHPG effect.

The role of mGluR5-mediated PLCβ1 activation and Ca²⁺ release

Gαq-coupled mGluR5 activates the predominant downstream effector PLCβ1. Active PLCβ1, in turn, increases PI hydrolysis to produce IP₃, which releases Ca^{2+} from intracellular Ca^{2+} stores (Nakanishi, 1994; Conn and Pin, 1997). Because mGluR5 mediates the DHPG action (see above), we set out to test whether mGluR5-sensitive PLCβ1 activation and $[Ca^{2+}]_i$ mobilization participate in transmitting mGluR5 signals to JNK. Surprisingly, the amino steroid inhibitor of PLCβ1, U73122 (40 μM), did not affect the DHPG (100 μM)-induced JNK phosphorylation (Fig. 4A) although U73122, but not its inactive analog U73343, totally blocked the DHPG (100 μM)-induced increase in PI hydrolysis (Fig. 4B). To test the involvement of Ca^{2+} release, a $[Ca^{2+}]_i$-depleting agent, thapsigargin (2 μM), was added 1 h before DHPG to discharge internal Ca^{2+} stores. Like U73122, thapsigargin did not alter the DHPG-induced JNK phosphorylation (Fig. 4C). Similar results were produced by using the cell-permeable Ca^{2+} chelators BAPTA-AM (30 μM) (Fig. 4D) and calcium green-1/AM (30 μM; data not shown). In the absence of extracellular Ca^{2+} ions, DHPG preserved its ability to induce robust JNK phosphorylation (Fig. 4E) and to increase $[Ca^{2+}]_i$ levels as measured by fura-2 AM fluorescence (Fig. 4F). Pretreatment with thapsigargin or BAPTA-AM blocked DHPG-induced $[Ca^{2+}]_i$ rises (Fig. 4F). These results appear to rule out the possibility of the conventional mGluR5-derived second messenger system (PLCβ1/IP₃/Ca^{2+}) to mediate mGluR5 signals to JNK. The mGluR5-mediated PLCβ1 activation also increases DCG, an

endogenous stimulator of PKC (Nakanishi, 1994; Conn and Pin, 1997). To determine the involvement of the DCG-PKC pathway, we examined the DHPG effect in the presence of PKC inhibitors. We found that DHPG retained its ability to stimulate JNK phosphorylation in the presence of the PKC inhibitor Ro-31–8220 (1 μM) (Fig. S3, available at www.jneurosci.org as supplemental material) or Gö6983 (1 μM). The two inhibitors at 1 μM effectively blocked the JNK phosphorylation induced by the PKC activator PMA (0.1 μM; 5 min) (Fig. S3, available at www.jneurosci.org as supplemental material). Thus, the DCG-PKC pathway is not a significant link in transmitting mGluR5 signals to JNK.

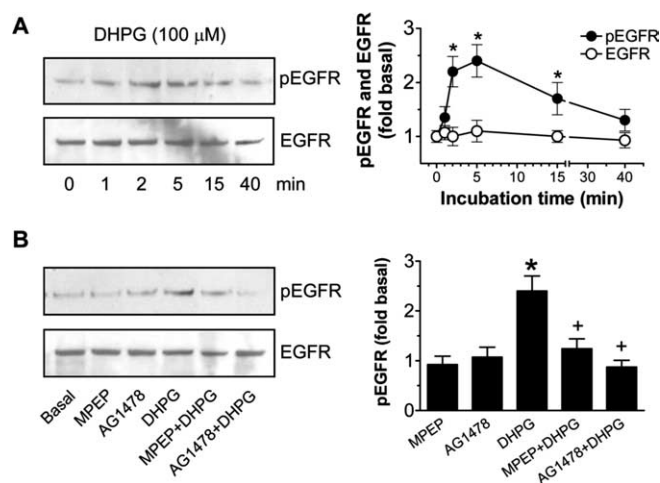### Transactivation of EGF receptors is required for mGluR5-mediated JNK phosphorylation

Given the absence of PLCβ1/Ca^{2+} involvement in the mGluR5-regulated JNK phosphorylation, we investigated the possible role of tyrosine kinases, a class of kinases often involved in the inducible ERK and JNK phosphorylation. EGF receptors (ErbB1) exhibit intrinsic protein tyrosine kinase activity and are expressed in striatal neurons of young rats (Fox and Kornblum, 2005). Stimulation of G-protein-coupled receptors engaging pertussis toxin (PTX)-insensitive G-proteins of the Gαq subclass and, to a lesser extent, PTX-sensitive G-proteins of the Gi subclass transactivated EGF receptors in COS-7 cells (Daub et al., 1997). Recent evidence shows that the EGF receptor tyrosine kinase mediates
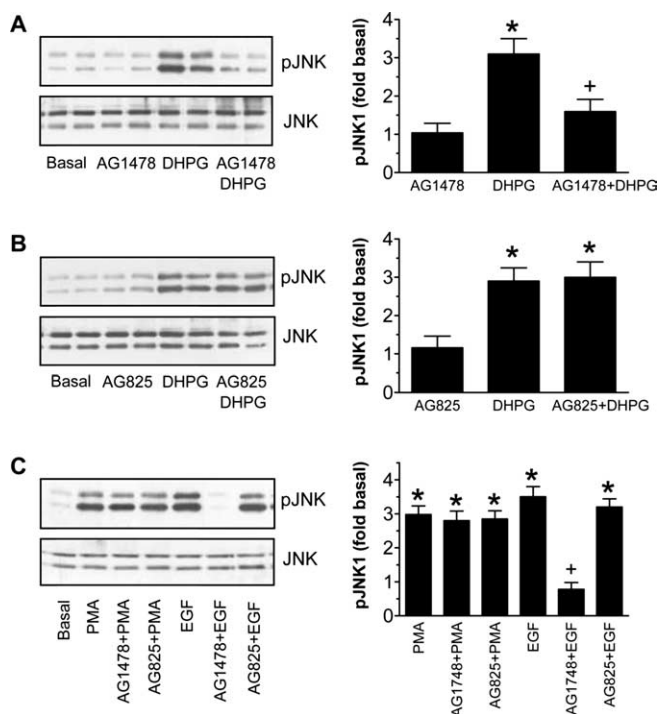
Figure 5. Effects of the EGF receptor inhibitor on the DHPG-induced JNK phosphorylation in cultured rat striatal neurons. **A**, The EGF ErbB1 receptor inhibitor AG1478 blocked the DHPG-induced JNK phosphorylation ($n = 6$). **B**, The ErbB2 receptor inhibitor AG825 did not affect the DHPG-induced JNK phosphorylation ($n = 3$). **C**, Effects of AG1478 or AG825 on the EGF- or PMA-induced JNK phosphorylation ($n = 4$). AG1478, but not AG825, blocked JNK phosphorylation induced by the recombinant human EGF. Both of the inhibitors had no effect on the PMA-stimulated JNK phosphorylation. Representative immunoblots are shown to the left of the quantified data of pJNK1. AG1478 or AG825 (0.1 μM) was incubated 15 min before and during a 10 min treatment with DHPG (100 μM), EGF (10 ng/ml), or PMA (1 μM). *$p < 0.05$ versus basal levels. $^+p < 0.05$ versus DHPG (**A**) or EGF (**C**) alone.

Figure 6. Transactivation of EGF receptors after mGluR5 stimulation in cultured rat striatal neurons. **A**, A time course study illustrating a rapid and transient increase in tyrosine 1173 phosphorylation of EGF receptors after DHPG incubation at 100 μM for different durations. No change in expression of EGF receptors was observed. Representative immunoblots are shown to the left of the quantified data (mean ± SEM; $n = 4$). **B**, The mGluR5 antagonist MPEP and the EGF receptor inhibitor AG1478 blocked the DHPG-induced tyrosine phosphorylation of EGF receptors. Representative immunoblots are shown to the left of the quantified data (mean ± SEM; $n = 4$). MPEP (1 μM) or AG1478 (0.1 μM) was incubated 15 min before and during a 10 min treatment with DHPG (100 μM). *$p < 0.05$ versus basal levels. $^+p < 0.05$ versus DHPG alone.

signals from Gαq-coupled receptors to ERK1/2 (Peavy et al., 2001). We therefore tested the possibility as to whether activation of mGluR5 could cause transactivation of EGF receptors to increase JNK phosphorylation. Interestingly, pretreatment with a tyrphostin AG1478 (0.1 μM), a selective inhibitor for EGF receptors (Levitzki and Gazit, 1995), blocked the DHPG-induced JNK phosphorylation (Fig. 5A). However, AG825 (0.1 μM), a related tyrphostin that selectively inhibits the related receptor tyrosine kinase ErbB2 (HER2/neu) with no effects on EGF receptors (ErbB1) (Osherov et al., 1993), did not alter the DHPG effect (Fig. 5B). Consistent with its ability to inhibit EGF receptors, AG1478 blocked the JNK phosphorylation induced by EGF (10 ng/ml; 10 min) (Fig. 5C). In contrast, AG1478 and AG825 had no effect on PMA (1 μM; 10 min)-induced JNK phosphorylation (Fig. 5C). These data demonstrated that the EGF receptor tyrosine kinase serves as an important effector in a signaling pathway connecting mGluR5 to JNK.

EGF receptors undergo a rapid, intramolecular dimerization and autophosphorylation at specific C-terminal tyrosine residues, including tyrosine 1173, after ligand activation (Downward et al., 1984; Boonstra et al., 1995). Activation of G-protein-coupled receptors also transactivates the EGF receptor by increasing its tyrosine autophosphorylation (Peavy et al., 2001). To further characterize the transactivation of EGF receptors by mGluR5, we measured the tyrosine phosphorylation of EGF receptors by using a phospho-specific antibody that recognizes the autophosphorylation site (tyrosine 1173) of the native EGF receptor from striatal neuronal lysates. DHPG (100 μM) induced a rapid and transient increase in the tyrosine phosphorylation of EGF receptors (Fig. 6A). The dynamic phosphorylation of EGF receptors paralleled well with the time course of the JNK phosphorylation induced by DHPG (compare Figs. 6A and 1C). Immunoblotting with the EGF receptor antibody showed no change in the overall expression of this receptor throughout the course of mGluR5 stimulation (Fig. 6A). The increase in tyrosine phosphorylation of EGF receptors was blocked by pretreatment with MPEP (1 μM) or AG1478 (0.1 μM) (Fig. 6B) but not with AG825, even at a higher concentration (1 μM). The above results support a signaling model that mGluR5 stimulation leads to transactivation of EGF receptors, which subsequently induces downstream JNK phosphorylation.

Agonist activation of G-protein-coupled β_2-adrenergic receptors facilitated a formation of a multiprotein complex of Src, the EGF receptor, and the β_2-adrenergic receptor, leading to activation of ERK1/2 (Maudsley et al., 2000). Activation of mGluR5 also promoted a similar complex formation to activate ERK1/2 in cortical astrocytes (Peavy et al., 2001). To determine whether mGluR5 stimulation promotes the physical association of mGluR5 with the EGF receptor in striatal neurons, a coimmunoprecipitation protocol was conducted in this culture system. Under basal conditions, a low level of EGF receptors was detected in mGluR5 immunoprecipitates and verse versa in a reverse coimmunoprecipitation. After DHPG stimulation (100 μM; 3–5 min), the amount of EGF receptors in mGluR5 immunoprecipitates was increased by 36% ($p < 0.05$). Similarly, the amount of mGluR5 was increased in EGF receptor immunoprecipitates by 40% ($p < 0.05$). These results suggest a dynamic formation of multiprotein complexes containing mGluR5 and EGF receptors for a function of transmitting mGluR5 signals to JNK.
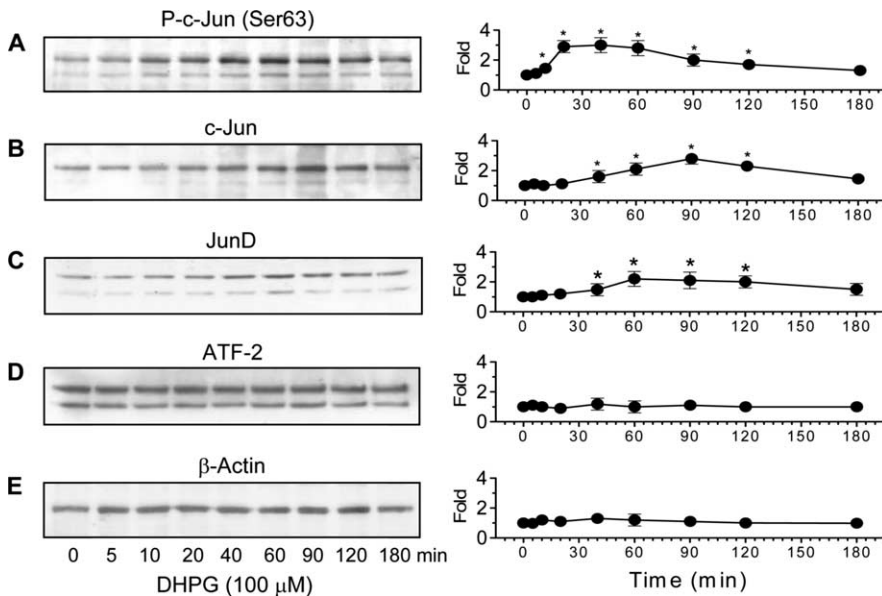
Figure 7. Effects of activation of mGluR5 with DHPG on phosphorylation and expression of key transcription factors downstream to the JNK pathway in cultured rat striatal neurons. DHPG increased cellular levels of phospho-c-Jun at serine 63 (**A**), c-Jun (**B**), and JunD (**C**) in a time-dependent manner. Total levels of ATF-2 (**D**) and β-actin (**E**) proteins remained unchanged throughout the time course surveyed. Western blots were probed with the indicated antibodies on the lysates from striatal cultures treated with DHPG at 100 μM for different durations. Representative immunoblots are shown to the left of the quantified data (mean $\pm$ SEM; $n = 3$–6). *$p < 0.05$ versus corresponding basal levels.
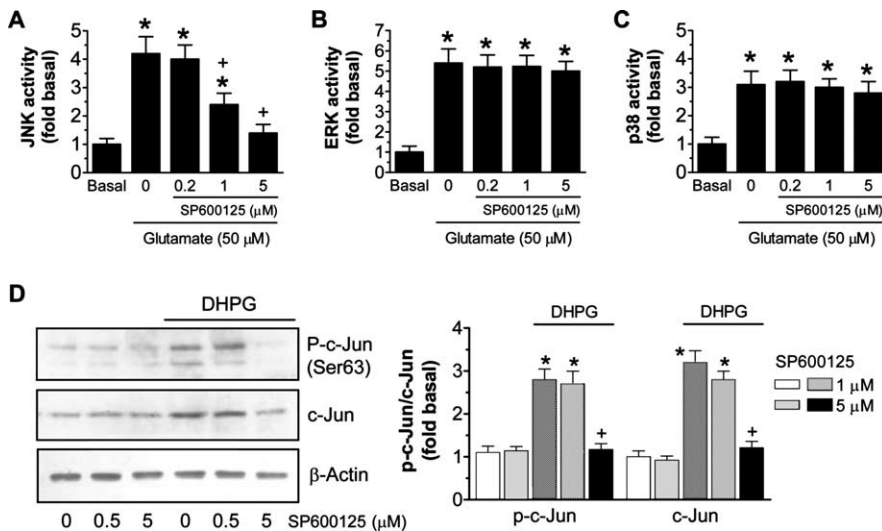
Figure 8. Effects of the JNK inhibitor SP600125 on the glutamate-stimulated JNK, ERK, and p38 activity and the DHPG-induced phosphorylation and expression of c-Jun in cultured rat striatal neurons. SP600125 concentration-dependently blocked the glutamate-stimulated JNK activity (**A**) but not ERK (**B**) or p38 (**C**) activity. Activity assays of the whole-cell fraction were conducted in striatal cultures treated with SP600125 (0.2, 1, or 5 μM) incubated 15 min before and during a 10 min treatment with glutamate (50 μM). **D**, SP600125 blocked the DHPG-stimulated phosphorylation and expression of c-Jun without changing total levels of β-actin. SP600125 was incubated 15 min before and during a 1.5 h treatment with DHPG (100 μM). Western blots were probed with the antibody against phospho-c-Jun(Ser63), c-Jun, or β-actin. Representative immunoblots are shown to the left of the quantified data (mean $\pm$ SEM; $n = 4$–5). *$p < 0.05$ versus basal levels. +$p < 0.05$ versus glutamate or DHPG alone.

Physiological roles of mGluR5-sensitive JNK signaling in regulating gene expression

One of the important functional roles that active JNK plays is to regulate gene expression (transcription) via phosphorylating distinct transcription factors (Wang et al., 2004). The transcription factors that JNK directly phosphorylates include the Jun family, c-Jun (Hibi et al., 1993; Derijard et al., 1994) and, to a lesser extent, JunD but not JunB (Karin, 1995; Kallunki et al., 1996),

and ATF-2 (Gupta et al., 1995, 1996). We then examined the profile of the mGluR5-regulated JNK pathway in phosphorylating these substrates. DHPG (100 μM) induced a dynamic increase in cellular levels of phospho-c-Jun(Ser63) proteins (Fig. 7A). This increase was sensitive to MPEP (1 μM) but not CPCCOet (5 μM). However, the same treatment with DHPG did not alter basal levels of phospho-ATF-2(Ser80) and phospho-JunD(Ser100) proteins (data not shown). It appears that the mGluR5-mediated JNK activation preferentially activates c-Jun rather than ATF-2 and JunD in striatal neurons.

Phospho-c-Jun is a principal dimer in assembling an active transcription factor, AP-1, in striatal neurons in response to glutamate stimulation (Schwarzschild et al., 1997). Given an increased expression of phospho-c-Jun proteins after DHPG stimulation, AP-1 activity could be elevated (see below) to upregulate the AP-1-mediated transcription. The promoter region of c-Jun and JunD contains the AP-1-binding element or the binding sites sharing homology with the consensus AP-1 element (Angel et al., 1988; Rozek and Pfeiffer, 1993). Thus, these genes are likely to be positively autoregulated by their product Jun/AP-1. In fact, total levels of c-Jun proteins exhibited a significant increase after DHPG stimulation (Fig. 7B), and so did JunD proteins (Fig. 7C). In contrast, basal expression of ATF-2 was not responsive to DHPG stimulation (Fig. 7D), despite the fact that the promoter region of this gene shows potential AP-1 binding sites (Kravets et al., 2004). It appears that activation of AP-1 via the mGluR5-dependent JNK/c-Jun pathway specifically facilitates endogenous c-Jun and JunD expression. In addition, it is noted that the increase in c-Jun phosphorylation preceded the increase in c-Jun expression. Thus, the increase in c-Jun phosphorylation should result from an increased phosphorylation modification of this protein at the early time points (10–20 min after DHPG treatment) when changes in total levels of c-Jun proteins have not yet occurred.

To directly assess the role of the JNK pathway in activating c-Jun, SP600125, a highly selective inhibitor of JNK1/2/3 (Bennett et al., 2001), was used to inactivate JNK. We first evaluated the selectivity of SP600125 in inhibiting JNK activity by probing kinase assays for JNK, ERK, and p38 at different drug concentrations. SP600125 (0.2–5 μM) significantly inhibited glutamate (50 μM)-induced JNK activity in a dose-dependent manner (Fig. 8A), although SP600125 did not alter the levels of pJNK because of its nature in selectively inhibiting kinase activity but not JNK phosphorylation (Bennett et al., 2001). The kinase activ-

ity of ERK or p38 was not altered in the presence of SP600125 (Fig. 8, *B*, ERK; *C*, p38). These results validate the selectivity and efficacy of SP600125 in inhibiting JNK activity in this model of striatal cultures. We then tested the effect of this agent on the DHPG-stimulated c-Jun phosphorylation and expression. We found that SP600125 (5 μM) blocked the DHPG-induced c-Jun phosphorylation and c-Jun protein expression (Fig. 8*D*). This result supports that the DHPG-induced c-Jun activation was dependent on activation of the upstream JNK pathway.

DHPG induces AP-1-mediated transcription via the JNK pathway

By analyzing activity of transfected luciferase driven by the AP-1-specific binding, we further evaluated endogenous AP-1-mediated transcription in cultured striatal neurons in response to group I mGluR stimulation. DHPG (1–100 μM) concentration-dependently elevated the activity of the luciferase reporter gene (Fig. 9*A*). In contrast, dopamine (1–100 μM) did not induce any significant increase in the luciferase activity (Fig. 9*A*), a similar result to that observed previously (Schwarzschild et al., 1997). Thus, activation of group I mGluRs can trigger AP-1-mediated transcription in living striatal cells. The DHPG-induced transcriptional activity was markedly reduced by pretreatment with either the mGluR5 antagonist MPEP (1 μM) or the JNK inhibitor SP600125 (5 μM) (Fig. 9*B*). In contrast, the mGluR1 antagonist CPCCOet (5 μM) did not alter the DHPG-induced transcriptional activation of AP-1-driven luciferase gene (Fig. 9*B*). Thus, the mGluR5-to-JNK pathway mediates the effect of DHPG on AP-1 transcription.

Discussion

The present study investigated the role of group I mGluRs in regulating the JNK pathway in cultured neurons. We found that selective stimulation of mGluR5 activated JNK. The JNK activation was not mediated by the mGluR5-associated conventional PLCβ1/IP$_3$/Ca^{2+} pathway. Interestingly, the mGluR5-regulated JNK activation primarily relies on transactivation of the EGF receptor tyrosine kinase that has an association with the C terminus of mGluR5. Furthermore, the mGluR5-dependent JNK activation leads to phosphorylation of c-Jun but not JunD or ATF-2. Phosphorylated c-Jun constitutes an enhancement of AP-1-mediated transcription, resulting in c-Jun and JunD protein expression. These results reveal a novel synapse-to-nucleus communication transmitting extracellular signals through mGluR5 to JNK and JNK-controlled transcription factors for the transcriptional regulation of target gene expression in cultured neurons.

The role of mGluRs, especially group I mGluRs, in the regulation of MAPKs, mainly the ERK subclass, in brain cells has been extensively investigated in recent years (Wang et al., 2004). A large number of reports have documented a significant influence of group I mGluRs, particularly mGluR5 subtype, in upregulating phosphorylation of ERK1/2 in various cell lines, glial cells, and neurons *in vitro* or *in vivo* (Ferraguti et al., 1999; Schinkmann et al., 2000; Choe and Wang, 2001a,b; Peavy et al., 2001; Thandi et al., 2002). As to the signaling pathway that mediates mGluR5
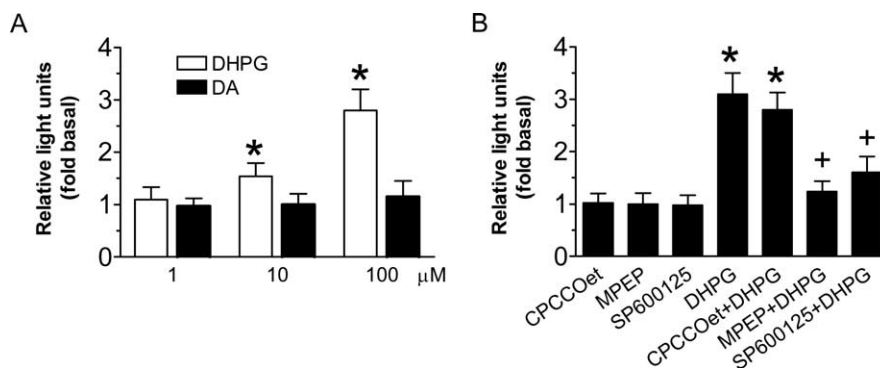
Figure 9. Effects of activation of group I mGluRs with DHPG on expression of a transfected AP-1 luciferase fusion construct in cultured rat striatal neurons. *A*, DHPG, but not dopamine (DA), activated transcription of an AP-1 luciferase construct. DHPG or dopamine at 1, 10, or 100 μM was added 18 h after transfection of the construct, and cells were harvested 2 h after DHPG or dopamine treatment for luciferase activity assay. *B*, The DHPG-induced AP-1 transcription was reduced by MPEP and SP600125 but not by CPCCOet. MPEP (1 μM), CPCCOet (5 μM), or SP600125 (5 μM) was added 30 min before the addition of DHPG (100 μM), and cells were harvested 2 h after the DHPG treatment for luciferase activity assay. Values for luciferase activity measured as RLUs are given as fold induction, and data are represented as mean ± SEM of percentage of transfected control values (*n* = 4). *$p <$ 0.05 versus basal levels. $^+p <$ 0.05 versus DHPG alone.

signals to ERK1/2, we and others have found that the mGluR5-regulated ERK1/2 phosphorylation has no or limited reliance on Ca^{2+} release derived from activation of the conventional PLCβ1/IP$_3$ pathway (Thandi et al., 2002; Mao et al., 2005). Instead, a Ca^{2+}-independent mechanism involving tyrosine kinases or mGluR5 scaffold proteins [Homer1b/c (Xiao et al., 2000)] links mGluR5 to ERK (Peavy et al., 2001; Mao et al., 2005). Compared with the well characterized ERK activation by mGluR5, the group I mGluR-specific regulation of another MAPK subclass JNK/SAPK has not been described previously in the nervous system. JNK, which was first cloned from fetal brain (Derijard et al., 1994; Kyriakis et al., 1994) as a critical mediator of responses to cellular stressors, inflammatory cytokines, and apoptosis (Derijard et al., 1994; Kyriakis and Avruch, 1996; Liu and Lin, 2005), has been found to be regulated by glutamatergic transmission (Schwarzschild et al., 1997; Mukherjee et al., 1999; Vanhoutte et al., 1999; Crossthwaite et al., 2004). It is therefore likely that this kinase could be an intracellular signaling molecule to be modulated by the group I mGluR-mediated glutamatergic transmission. The present work first demonstrated that mGluR5 in fact upregulated JNK phosphorylation. This upregulation occurred in striatal neurons and shares many common characteristics shown in the glutamate-sensitive JNK or ERK phosphorylation in different cell types. First, the time profile of the DHPG effect indicates a rapid and transient nature of the JNK hyperphosphorylation. Second, the noticeable distribution pattern of immunostaining showed a prime localization of pJNK in the nuclear compartment, indicating a role of pJNK in regulating gene expression. Third, basal levels of unphosphorylated JNK remained unchanged. Thus, the elevation of cellular levels of pJNK results from an increase in the phosphorylation modification of JNK. This is further supported by the concomitant activation of MKK4, an immediate upstream kinase phosphorylating JNK. Finally, the mGluR5-regulated JNK phosphorylation was insensitive to TTX. Thus, DHPG is believed to directly interact with the receptors on striatal neurons to facilitate JNK phosphorylation.

The signaling mechanism identified in this work for mediating mGluR5 phosphorylation of JNK is intriguing. We first noted that the DHPG-stimulated JNK activation was not dependent on extracellular Ca^{2+} ions and transmembrane Ca^{2+} influx through either ligand- or voltage-operated Ca^{2+} channels, because the

antagonists for ligand-gated Ca^{2+} channels (NMDA or AMPA receptors) or the inhibitor for voltage-gated Ca^{2+} channels did not affect JNK activation by DHPG. Moreover, DHPG stimulated JNK phosphorylation in the absence of extracellular Ca^{2+} ions. We subsequently found that the DHPG-stimulated JNK phosphorylation did not rely on intracellular Ca^{2+} release, a major conventional signaling event after mGluR5/PLCβ1/IP$_3$ stimulation. This is based on a series of observations obtained in this study. The PLCβ1 inhibitor U73122 did not change the DHPG-stimulated JNK phosphorylation. Neither did the $[Ca^{2+}]_i$-depleting agent thapsigargin and the cell-permeable Ca^{2+} chelators (BAPTA-AM and calcium green-1/AM). In the face of an unfavorable role of Ca^{2+} signals in the DHPG effect, we then explored the other possible mechanism(s). EGF receptors with the intrinsic protein tyrosine kinase activity are recently shown to be transactivated by Gαq-protein-coupled receptors in COS-7 cells and to convey signals from these receptors to ERK (Daub et al., 1997; Luttrell et al., 1999; Peavy et al., 2001). Thus, EGF receptors could be a candidate effector downstream to mGluR5 for mediating mGluR5 signals to JNK. Indeed, the findings from this study are in favor of this assumption. It was observed that: (1) the EGF receptor-selective inhibitor AG1478 blocked the DHPG-stimulated JNK phosphorylation; (2) DHPG transactivated EGF receptors through increasing tyrosine autophosphorylation of the receptors and the increased tyrosine phosphorylation of EGF receptors corresponded well with the kinetics of JNK phosphorylation; and (3) the association of EGF receptors with mGluR5 was increased after DHPG stimulation. Together, our data support a sequential signaling model, in which stimulation of Gαq-coupled mGluR5 induces transactivation of EGF receptors. Active EGF receptors could in turn increase the assembly of Shc-Grb2-SoS complexes and activate the Ras-Rac mitogenic pathway, leading to JNK activation.

One of the noticeable roles that active JNK plays is to regulate constitutive and inducible gene expression. After activation, the cytoplasmic JNK translocates into the nuclear compartment to perform such a function (Gupta et al., 1996; Kim and Kahn, 1997). There are a number of various extracellular signals that can regulate gene expression through the JNK superhighway. In this study, a high level of pJNK was seen within the nucleus envelop after mGluR5 stimulation, indicating a potential role in regulating gene expression. In the further attempt of clarifying this potential, we found that the mGluR5 agonist-induced JNK phosphorylation kinetically paralleled with increased phosphorylation of transcription factor c-Jun and expression of c-Jun/JunD. Moreover, selective inhibition of the JNK pathway with SP600125 abolished phosphorylation and expression of endogenous c-Jun. SP600125 and MPEP blocked the DHPG-induced transcriptional activation of AP-1-driven luciferase gene. These results demonstrated that mGluR5-dependent activation of the JNK pathway leads to a significant increase in AP-1-mediated transcriptional activity.

Active JNK phosphorylates a set of discrete transcription factors, including c-Jun (Hibi et al., 1993; Derijard et al., 1994), JunD (Kallunki et al., 1996), and ATF-2 (Gupta et al., 1995, 1996). The phosphorylation of these factors by JNK in terms of the selection and extent is determined by many conditions, including natures of extracellular signals and cell types. Our results showed that mGluR5-specific signals distinctively increased phosphorylation of c-Jun but not JunD and ATF-2. Thus, the mGluR5-mediated JNK activation has a high preference over phosphorylating c-Jun. The phosphorylated c-Jun could then lead to activation of the transcription factor AP-1 to facilitate target gene expression. Although the dimeric AP-1 can be assembled differentially from members of two families, the Fos-family (comprising c-Fos, Fra-1, Fra-2, and Fos-B) and the Jun-family (including c-Jun, Jun-D, and Jun-B) (Angel and Karin, 1991), it was found that the glutamate-activated AP-1 in striatal neurons was comprised by phosphorylated c-Jun proteins but not by JunB, c-Fos, FosB, or Fra-1 proteins (Schwarzschild et al., 1997). Thus, phosphorylated c-Jun in this culture model could be a major element in constituting an active AP-1 factor in response to mGluR5 stimulation.

References

Angel P, Karin M (1991) The role of Jun, Fos and the AP-1 complex in cell-proliferation and transformation. Biochim Biophys Acta 1072:129–157.

Angel P, Hattori K, Smeal T, Karin M (1988) The Jun proto-oncogene is positively autoregulated by its product Jun/AP-1. Cell 55:875–885.

Bennett BL, Sasaki DT, Murray BW, O'Leary EC, Sakata ST, Xu W, Leisten JC, Motiwala A, Pierce S, Satoh Y, Bhagwat SS, Manning AM, Anderson DW (2001) SP600125, an anthrapyrazolone inhibitor of Jun N-terminal kinase. Proc Natl Acad Sci USA 98:13681–13686.

Boonstra J, Rijken P, Humbel B, Cremers F, Verkleij A, van Bergen en Henegouwen P (1995) The epidermal growth factor. Cell Biol Int 19:413–430.

Choe ES, Wang JQ (2001a) Group I metabotropic glutamate receptor activation increases phosphorylation of cAMP response element-binding protein, Elk-1 and extracellular signal-regulated kinases in rat dorsal striatum. Mol Brain Res 94:75–84.

Choe ES, Wang JQ (2001b) Group I metabotropic glutamate receptors control phosphorylation of CREB, Elk-1 and ERK via a CaMKII-dependent pathway in rat striatum. Neurosci Lett 313:129–132.

Conn PU, Pin JP (1997) Pharmacology and function of metabotropic glutamate receptors. Annu Rev Pharmacol Toxicol 37:205–237.

Crossthwaite AJ, Valli H, Williams RJ (2004) Inhibiting Src family tyrosine kinase activity blocks glutamate signalling to ERK1/2 and Akt/PKB but not JNK in cultured striatal neurons. J Neurochem 88:1127–1139.

Daub H, Wallasch C, Lankenau A, Herrlich A, Ullrich A (1997) Signal characteristics of G protein-transactivated EGF receptor. EMBO J 16:7032–7044.

Derijard B, Hibi M, Wu IH, Barrett T, Su B, Deng T, Karin M, Davis RJ (1994) JNK1: a protein kinase stimulated by UV light and Ha-Ras that binds and phosphorylates the c-Jun activation domain. Cell 76:1025–1037.

Downward J, Parker P, Waterfield MD (1984) Autophosphorylation sites on the epidermal growth factor receptor. Nature 311:483–485.

Ferraguti F, Baldini-Guerra B, Corsi M, Nakanishi S, Corti C (1999) Activation of the extracellular signal-regulated kinase 2 by metabotropic glutamate receptors. Eur J Neurosci 11:2073–2082.

Fox IJ, Kornblum HI (2005) Developmental profile of ErbB receptors in murine central nervous system: implications for functional interactions. J Neurosci Res 79:584–597.

Gallo KA, Johnson GL (2002) Mixed-lineage kinase control of JNK and p38 MAPK pathways. Nat Rev Mol Cell Biol 3:663–672.

Gupta S, Campbell D, Derijard B, Davis RJ (1995) Transcription factor ATF2 regulation by the JNK signal transduction pathway. Science 267:389–393.

Gupta S, Barrett T, Whitmarch AJ, Cavanagh J, Sluss HK, Derijard B, Davis RJ (1996) Selective interaction of JNK protein kinase isoforms with transcription factors. EMBO J 15:2760–2770.

Hibi M, Lin A, Smeal T, Minden A, Karin M (1993) Identification of an oncoprotein- and UV- responsive protein kinase that binds and potentiates the c-Jun activation domain. Genes Dev 7:2135–2148.

Jones KH, Senft JA (1985) An improved method to determine cell viability by simultaneous staining with fluorescein diacetate-propidium iodide. J Histochem Cytochem 33:77–79.

Kallunki T, Deng T, Hibi M, Karin M (1996) c-Jun can recruit JNK to phosphorylate dimerization partners via specific docking interactions. Cell 87:929–939.

Karin M (1995) The regulation of AP-1 activity by mitogen-activated protein kinases. J Biol Chem 270:16483–16486.

Kim SJ, Kahn CR (1997) Insulin regulation of mitogen-activated protein

kinase kinase (MEK), mitogen-activated protein kinase and casein kinase in the cell nucleus: a possible role in the regulation of gene expression. Biochem J 323:621–627.

Kravets A, Hu Z, Miralem T, Torno MD, Maines MD (2004) Biliverdin reductase, a novel regulator for induction of activating transcription factor-2 and heme oxygenase-1. J Biol Chem 279:19916–19923.

Kyriakis JM, Avruch J (1996) Sounding the alarm: protein kinase cascades activated by stress and inflammation. J Biol Chem 271:24313–24316.

Kyriakis JM, Banerjee P, Nikolakaki E, Dal T, Ruble EA, Ahmad MF, Avruch J, Woodgett JR (1994) The stress-activated protein kinase subfamily of c-Jun kinase. Nature 369:156–160.

Levitzki A, Gazit A (1995) Tyrosine kinase inhibition: an approach to drug development. Science 267:1782–1788.

Liu J, Lin A (2005) Role of JNK activation in apoptosis: a double-edged sword. Cell Res 15:36–42.

Luttrell LM, Daaka Y, Lefkowitz RJ (1999) Regulation of tyrosine kinase cascades by G-protein-coupled receptors. Curr Opin Cell Biol 11:177–183.

Mao L, Wang JQ (2002) Glutamate cascade to cAMP response element-binding protein phosphorylation in cultured striatal neurons through calcium-coupled group I mGluRs. Mol Pharmacol 62:473–484.

Mao L, Tang Q, Samdani S, Liu Z, Wang JQ (2004) Regulation of MAPK/ERK phosphorylation via ionotropic glutamate receptors in cultured rat striatal neurons. Eur J Neurosci 19:1207–1216.

Mao L, Yang L, Tang Q, Samdani S, Zhang G, Wang JQ (2005a) The scaffold protein Homer1b/c links metabotropic glutamate receptor 5 to extracellular signal-regulated protein kinase cascades in neurons. J Neurosci 25:2741–2752.

Mao L, Yang L, Arora A, Choe ES, Zhang G, Liu Z, Kingston K, Fibuch E, Wang JQ (2005b) Role of protein phosphatase 2A in mGluR5-regulated MAPK/ERK phosphorylation in neurons. J Biol Chem 280:12602–12610.

Maudsley S, Pierce KL, Zamah AM, Miller WE, Ahn S, Daaka Y, Lefkowitz RJ, Luttrell LM (2000) The β2-adrenergic receptor mediates extracellular signal-regulated kinase activation via assembly of a multi-receptor complex with the epidermal growth factor receptor. J Biol Chem 275:9572–9580.

Mukherjee PK, DeCoster MA, Campbell FZ, Davis RJ, Bazan NG (1999) Glutamate receptor signaling interplay modulates stress-sensitive mitogen-activated protein kinases and neuronal cell death. J Biol Chem 274:6493–6498.

Nakanishi S (1994) Metabotropic glutamate receptors: synaptic transmission, modulation, and plasticity. Neuron 13:1031–1037.

Nozaki K, Nishimura M, Hashimoto N (2001) Mitogen-activated protein kinases and cerebral ischemia. Mol Neurobiol 23:1–19.

Osherov N, Gazit A, Gilon C, Levitzki A (1993) Selective inhibition of the epidermal growth factor and HER2/neu receptors by tyrphostins. J Biol Chem 268:11134–11142.

Pearson G, Robinson F, Gibson BT, Xu BE, Karandikar M, Berman K, Cobb MH (2001) Mitogen-activated protein (MAP) kinase pathways: regulation of physiological functions. Endo Rev 22:153–183.

Peavy RD, Chang MSS, Sanders-Bush E, Conn PJ (2001) Metabotropic glutamate receptor 5-induced phosphorylation of extracellular signal-regulated kinase in astrocytes depends on transactivation of the epidermal growth factor receptor. J Neurosci 21:9619–9628.

Perkinton MS, Sihra TS, Williams RJ (1999) Ca^{2+}-permeable AMPA receptors induce phosphorylation of cAMP response element-binding protein

through a phosphatidylinositol 3-kinase-dependent stimulation of the mitogen-activated protein kinase signaling cascade in neurons. J Neurosci 19:5861–5874.

Perkinton MS, Ip JK, Wood GL, Crossthwaite AJ, Williams RJ (2002) Phosphatidylinositol 3-kinase is a central mediator of NMDA receptor signalling to MAP kinase (Erk1/2), Akt/PKB and CREB in striatal neurons. J Neurochem 80:239–254.

Peyssonnaux C, Eychene A (2001) The Raf/MEK/ERK pathway: new concepts of activation. Biol Cell 93:53–62.

Rozek D, Pfeiffer GP (1993) In vivo protein-DNA interactions at the c-jun promoter: preformed complexes mediate the UV response. Mol Cell Biol 13:5490–5499.

Schinkmann KA, Kim TA, Avraham S (2000) Glutamate stimulated activation of DNA synthesis via mitogen-activated protein kinase in primary astrocytes: involvement of protein kinase C and related adhesion focal tyrosine kinase (Pyk2). J Neurochem 74:1931–1940.

Schwarzschild MA, Cole RL, Hyman SE (1997) Glutamate, but not dopamine, stimulates stress-activated protein kinase and AP-1-mediated transcription in striatal neurons. J Neurosci 17:3455–3466.

Sgambato V, Vanhoutte P, Pages C, Rogard M, Hipskind R, Besson MJ, Caboche J (1998) In vivo expression and regulation of Elk-1, a target of the extracellular-regulated kinase signaling pathway, in the adult rat brain. J Neurosci 18:214–226.

Takagi N, Logan R, Teves L, Wallace MC, Gurd JW (2000) Altered interaction between PSD-95 and the NMDA receptor following transient global ischemia. J Neurochem 74:169–178.

Tallaksen-Greene SJ, Kaatz KW, Romano C, Albin RL (1998) Localization of mGluR1a-like immunoreactivity and mGluR5-like immunoreactivity in identified population of striatal neurons. Brain Res 780:210–217.

Testa CM, Standaert DG, Young AB, Penney Jr JB (1994) Metabotropic glutamate receptor mRNA expression in the basal ganglia of the rat. J Neurosci 14:3005–3018.

Thandi S, Blank JL, Challiss RA (2002) Group I metabotropic glutamate receptors, mGluR1a and mGluR5 couple to extracellular signal-regulated kinase (ERK) activation via distinct, but overlapping, signaling pathways. J Neurochem 83:1139–1153.

Vanhoutte P, Barnier JV, Guibert B, Pages C, Besson MJ, Hipskind RA, Caboche J (1999) Glutamate induces phosphorylation of Elk-1 and CREB, along with c-fos activation, via an extracellular signal-regulated kinase-dependent pathway in brain slices. Mol Cell Biol 19:136–146.

Volmat V, Pouyssegur J (2001) Spatiotemporal regulation of the p42/p44 MAPK pathway. Biol Cell 93:71–79.

Wang JQ, Mao L, Parelkar NK, Tang Q, Liu Z, Sarwar S, Choe ES (2003) Glutamate-regulated behavior, transmitter release, gene expression and addictive plasticity in the striatum: roles of metabotropic glutamate receptors. Curr Neuropharmacol 1:1–20.

Wang JQ, Tang Q, Samdani S, Liu Z, Parelkar NK, Choe ES, Yang L, Mao L (2004) Glutamate signaling to Ras-MAPK in striatal neurons: mechanisms for inducible gene expression and plasticity. Mol Neurobiol 29:1–14.

Xiao B, Tu JC, Worley PF (2000) Homer: a link between neural activity and glutamate reception. Curr Opin Neurobiol 10:370–374.

Yang L, Mao L, Tang Q, Samdani S, Liu Z, Wang JQ (2004) A novel Ca^{2+}-independent signaling pathway to extracellular signal-regulated protein kinase by coactivation of NMDA receptors and metabotropic glutamate receptor 5. J Neurosci 24:10846–10857.